

Flight Results from a Novel Magnetic Actuator on the LatinSat Spacecraft

Doug Sinclair

Sinclair Interplanetary, 27 Wandering Trail Drive, Brampton, Ontario, Canada, L7A 1T5

Tel: (905) 495-0448

dns@sinclairinterplanetary.com

Dr. Chris Damaren

University of Toronto, Institute for Aerospace Studies, 4925 Dufferin St, Toronto, Ontario, Canada, M3H 5T6

Tel: (416) 667-7704

damaren@utias.utoronto.ca

Abstract. The LatinSat-A and -B spacecraft were launched into low Earth orbit in December of 2002. Built by SpaceQuest, these 11 kg microsattellites carry commercial UHF payloads. Their attitude control systems employ a novel magnetic actuator that can provide large torques while using very little power.

At the core of the device is a rod of Alnico alloy, capable of storing a 13 Am² magnetic dipole. Copper windings around this rod connect to a high-voltage pulse generator. High power pulses can degauss or permanently reverse the polarity of the magnet. A hall-effect sensor provides magnetic field telemetry to the flight computer, and allows for closed-loop control. Once the polarity of the rod is set, no additional power is required to maintain it.

Previous SpaceQuest microsattellites have used permanent magnets in their ACS to align them with the Earth's field. These spacecraft complete two pitch rotations per orbit, so that the side that faces the Earth over the northern hemisphere faces space over the southern hemisphere. The LatinSats can degauss and then reverse their magnets each time they pass over the magnetic equator. This should allow a single side to face the Earth at all times.

Introduction

Satellites in low Earth orbit have long used magnetic dipoles to control their attitudes. Traditionally, these fields are created by either permanent magnets, or by electromagnets. Permanent magnets are cheap and simple, but cannot be controlled. Electromagnets, also known as magnetic torquers, are as flexible as their drive circuits. They may be turned on and off, reversed, and potentially driven linearly. However, they require the continual input of electric current to maintain a fixed dipole.

Over the past twelve months, Sinclair Interplanetary has developed a spacecraft magnetic actuator that combines the best qualities of a permanent magnet and an electromagnet. It can be turned on and off, reversed, and commanded to any fraction of its maximum dipole. Once the desired magnetic field is reached, no further electrical power is required to maintain it. This new technology is called a *reversible permanent magnet*.

Two reversible permanent magnets are presently on-orbit on LatinSat-A and LatinSat-B. Another flight unit has been integrated with the AMSAT-OSCAR-E satellite and is awaiting launch. These spacecraft are magnetically stabilized.

The actuator allows them to flip-over and present the opposite face to the Earth.

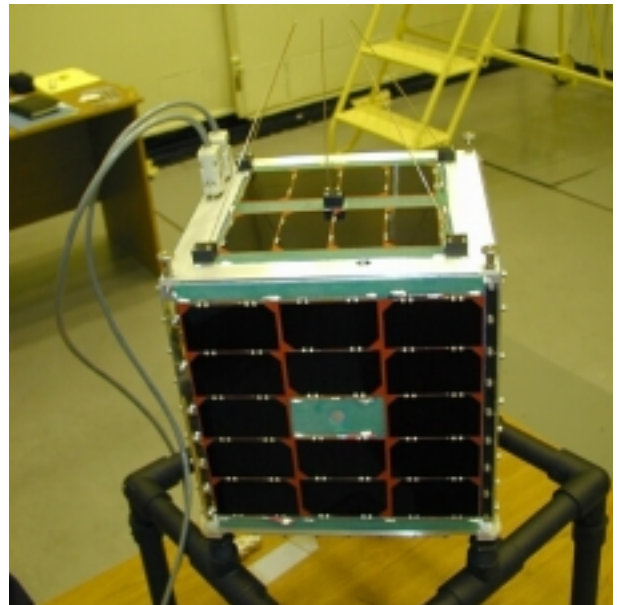


Figure 1: One of the LatinSat Spacecraft

LatinSat

LatinSat-A and LatinSat-B are the first two operational satellites in the LatinSat Network. Operated by Aprize Satellite Inc. and built by SpaceQuest Ltd., these spacecraft offer commercial tracking and monitoring services. Messages from transponders in remote locations are stored on-board, and then retransmitted to the network operations center. Applications include monitoring the level of fuel tanks and tracking the location of trailers, containers and rail cars.

Table 1: LatinSat Specifications

Manufacturer	SpaceQuest Ltd.
Number of Satellites	Two
Launch Date	December 20, 2002
Launcher	SS-18 Dnepr
Orbit	650 x 650 km (LatinSat-A) 650 x 700 km (LatinSat-B) 64.5° Inclination
Mass	11 kg
Power	6 GaAs solar panels NiCd rechargeable battery
TT&C	UHF command and telemetry
Primary Payload	UHF commercial store-and-forward transponder
Secondary Payload	Xiphos Q4 controller experiment (LatinSat-B only)
ACS Equipment	Reversible permanent magnet Backup magnet Hysteresis rods Black and silver spin tape 3-axis rate sensor (LatinSat-B only) 3-axis magnetometer (LatinSat-B only) 3-axis accelerometer (LatinSat-B only)

All communications, both for TT&C and payload functions, are performed in the UHF band. One set of antennas is on the +Z (top) face, while another set is on the -Z face. The pyramid arrays of the circularly-polarized antenna elements can be seen in Figure 1. The antenna gains are omnidirectional, so that each antenna has an approximately hemispherical radiation pattern.

Each of the six sides of the spacecraft has a gallium-arsenide solar array so that electrical power can be generated in any attitude. There are no other devices that are dependent on orientation, so the only attitude control requirements come from the desire to point one of the antennas at the Earth and to manage the spin rate.

The reversible permanent magnet is used to align the spacecraft Z-axis with the Earth's magnetic field. This keeps one set of antennas pointed towards Earth over the northern hemisphere, and the other pointed towards Earth over the southern hemisphere. By reversing the magnetic polarity, the satellite orientation can be flipped.

Asymmetric black and silver tape placed on the ends of each side of the spacecraft produces a Z-axis torque from the solar pressure effect. This causes the satellite to spin about the local magnetic field line. Seven magnetic hysteresis rods in the X-axis damp libration motion. They also prevent the spin rate from becoming too high.

A small permanent magnet, also aligned with the Z-axis, is used as a backup to the reversible permanent magnet. In the very unlikely event that the reversible magnet became completely degaussed and could not be recovered, the smaller magnet would maintain pointing. With the success of these missions, the backup will be removed from future satellites.

The LatinSat ACS is conducted entirely feed-forwards, and no sensors are required. Nevertheless, the current telemetry from the six solar arrays can be used as a crude full-sky sun sensor. LatinSat-B also carries a Q4 Controller experiment, built by Xiphos Technologies Inc. and sponsored by the Canadian Space Agency. While primarily a communications experiment, the Q4 features 3-axis magnetometers, rate sensors and accelerometers.

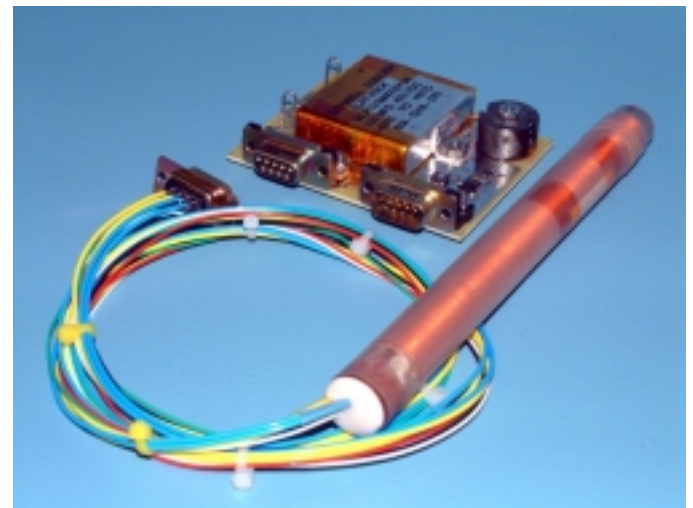


Figure 2: Magnet Rod and Drive Electronics

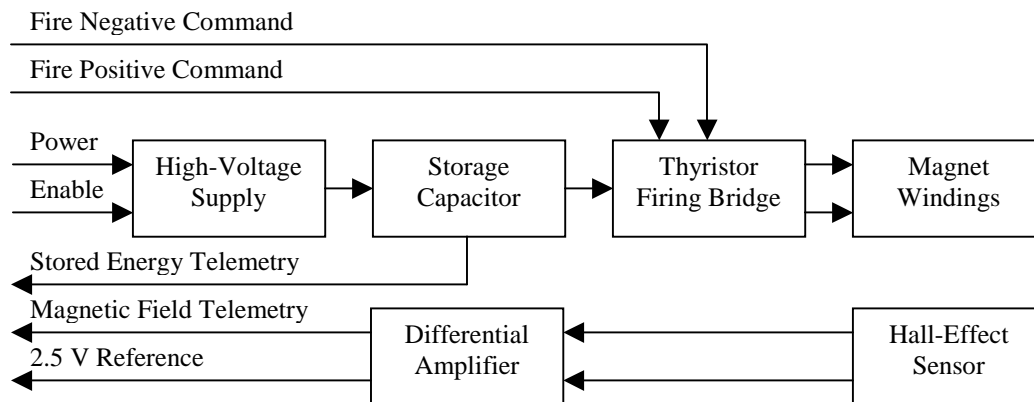


Figure 3: Actuator Block Diagram

The Actuator

At the heart of the reversible permanent magnet is a rod of Alnico-5. The name of the alloy is derived from its composition: 8% aluminum, 14% nickel, 24% cobalt, 3% copper, and 51% iron¹. The rods are heat-treated in an intense magnetic field to produce an anisotropic structure that favours an axial dipole. Alnico is familiar as the red-painted magnets in any high-school science lab.

The dipole of the rod may be permanently affected by passing a current through a solenoid winding. To achieve a sizeable change at least 10,000 amp-turns are required. This is completely impractical at steady state. The windings would overheat and the power draw from the spacecraft would be too great. However, the current need only last for 100 μ sec to permanently change the rod dipole. While the peak power is measured in kilowatts, the total pulse energy is measured in joules.

Table 2: Reversible Permanent Magnet Specifications

Manufacturer	Sinclair Interplanetary
Drive electronics	79 mm x 61 mm x 19 mm 80 grams
Magnet rod	16.6 mm \varnothing x 165 mm 230 grams
Command inputs	Enable Fire positive Fire negative
Telemetry outputs	Magnetic field Stored energy Reference voltage
Maximum pulse energy	2.6 Joules
Instantaneous pulse power	> 10 kW
Pulse dipole change	$\pm 4.5 \text{ Am}^2$ (starting from zero field)
Saturation dipole	> $\pm 13 \text{ Am}^2$

The second part of the reversible permanent magnet system is the drive electronics board. This must store several joules of energy and release it in a fraction of a millisecond. A high-voltage electrolytic capacitor proves to be the only practical storage device. Magnetic storage, as in an inductor, would be far too bulky. Super-capacitors have outstanding energy density, but cannot meet the peak power requirements. A high-voltage capacitor with hermetic seals is selected to ensure a long life in the space environment.

The capacitor is charged by a DC-DC converter, running from the spacecraft battery. It uses a quasi-resonant flyback topology operating as a constant-current source with a maximum voltage limit. In the LatinSat configuration the output power is set to 200 mW, so 13 seconds is required to store the full 2.6 J.

The technology used to switch the discharge pulse must also be carefully chosen. The devices must withstand high voltage in the OFF state, and very high current in the ON state. They must also switch quickly, and fit inside a limited envelope. MOSFETs with an acceptable die area have unacceptable resistance. Bipolar transistors have very low gain at this level of current. The choice for LatinSat is the thyristor. This device, not often seen in modern spacecraft, can withstand high voltages in the OFF state. In the ON state, a controlled breakdown with positive feedback allows extremely high currents with minimal voltage drop. The only complication is that the thyristor cannot be turned OFF by external command. It will only reset itself after the capacitor charge has been completely exhausted.

The thyristors are configured in an H-bridge, so that current may be commanded to flow in either direction in the magnet windings. A lockout circuit prevents both halves of the bridge from conducting simultaneously, which would result in a short-circuit.

At the tip of the magnet rod is a tiny Hall-effect sensor. This measures the axial magnetic field. An amplifier on the drive electronics board conditions the signal and sends it to the spacecraft telemetry system. By measuring the magnetic field, the total dipole moment of the rod may be estimated.

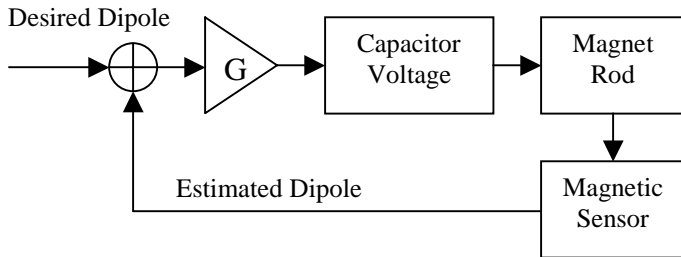


Figure 4: Closed-Loop Control

The reversible permanent magnet may be operated by the host spacecraft in a closed-loop mode. The measured dipole is compared to the desired value, and a corrective pulse energy is determined. The high-voltage supply is enabled, and the capacitor voltage is monitored. When the capacitor reaches the appropriate level, the supply is disabled and the thyristor bridge is fired with the desired polarity. The resulting magnetic field is measured with the Hall-effect sensor and the cycle repeats.

Background

Table 3: Magnetically Stabilized Microsatellites

<i>Launch Date</i>	<i>Satellites</i>	<i>ACS Hardware</i>
1962 to 1969	SECOR program ² (13 total)	Hysteresis Rods, Magnet
1967	TETR-1	Hysteresis Rods, Magnet
1968	TETR-2	
1969	TETR-3	
1971	TETR-4	
1970	OSCAR-5	Hysteresis Rods, Magnet
1972	OSCAR-6	
1974	OSCAR-7	Hysteresis Rods, Magnet, Spin Tape
1978	OSCAR-8	
1990	PACSAT WEBER DOVE LUSAT	Hysteresis Rods, Magnet, Spin Tape
1993	ITAMSAT EYESAT	Hysteresis Rods, Magnet, Spin Tape
2000	SaudiSat-1A SaudiSat-1B	Hysteresis Rods, Magnet, Spin Tape
2000	Munin	Hysteresis Rods, Magnet
2002	SaudiSat-1C	Hysteresis Rods, Magnet, Spin Tape
2002	LatinSat-1A LatinSat-1B	Hysteresis Rods, Magnet, Spin Tape, Reversible Permanent Magnet

Table 3 is a non-exhaustive list of microsatellites that have used magnets as their primary attitude control device. It shows that this technique has been used since the dawn of the space age, largely without incident. Many of the upcoming Cubesat missions also use permanent magnets. An excellent description of the attitude results for the 1990 AMSAT microsatellites was written by White³.

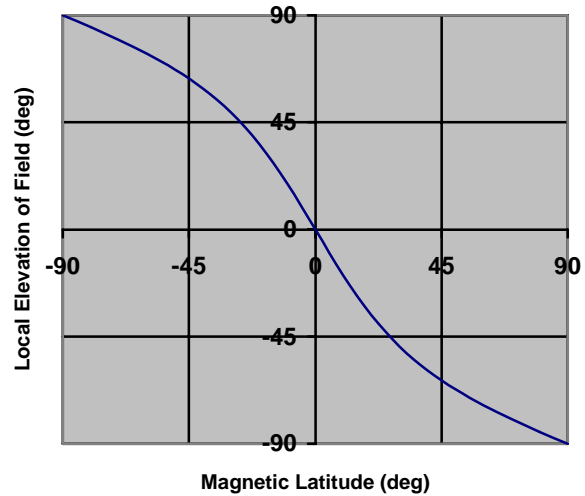


Figure 5: Local Elevation of Geomagnetic Field

Figure 5 shows the elevation of the local geomagnetic field, assuming a simple dipole model. In the northern magnetic hemisphere, the geomagnetic field lines come down from the sky into the Earth and so their elevation is considered negative. In the southern hemisphere, the situation is reversed. Exactly at the magnetic equator the geomagnetic field lines are perfectly horizontal.

Magnetically stabilized satellites typically have their Z-axes aligned with the geomagnetic field. Over the North pole, their +Z faces will point towards the Earth. They stay close to Earth pointing down to low-latitudes; at 30° north they point to within 45° of the nadir. Over the equator, they execute a rapid 180° flip so that their -Z faces now point towards the Earth. A satellite that communicates only with ground stations in the northern magnetic hemisphere would require a single TT&C antenna on its +Z face.

With the Z-axis aligned with the Earth’s magnetic field, the satellite is still free to spin about this line. Such a rotation is often desired to help balance the thermal loads on the spacecraft. A small Z-axis torque is provided by intentionally unbalancing the solar radiation pressure. Asymmetric patterns of black and silver tape on solar arrays or antennas slowly cause the satellite to spin.

A magnet alone provides no damping and librations about the geomagnetic field lines would be expected. Damping is

usually provided by magnetic hysteresis rods in an orthogonal axis. These react against libration in one axis and tend to pull energy out of the system. It is important to note that there can be no damping about the local field line. Therefore, if the satellite is truly aligned with the field, there can be no damping of the solar-pressure induced Z-axis spin. Nevertheless, the orbital spin rate has been observed to be a function of the strength of the hysteresis damper.

This must be because the Z-axis is in fact not aligned perfectly with the geomagnetic field. The spin provides a gyroscopic stiffness, and causes the Z-axis to slightly lag the geomagnetic field. The misalignment then means that the hysteresis rods can react against a small component of the spin.

Pre-Launch Results

Before it was shipped to SpaceQuest, the LatinSat ACS hardware underwent acceptance testing. Some of the more relevant data from the LatinSat-B hardware is shown here.

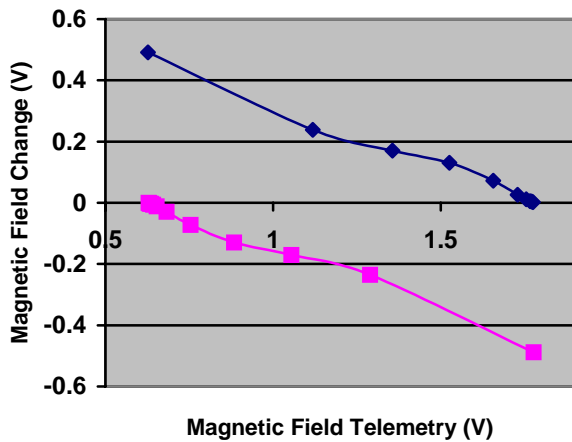


Figure 6: LatinSat-B Full Power Pulse Response

Figure 6 shows the effect on magnetic field from a single pulse. The horizontal axis is the magnetic field before the pulse is fired, and the vertical axis is the change in the field after the pulse. The top curve shows the effect of positive pulses, while the bottom curve indicates negative pulses.

The graph shows the range of fields that can be reached as 0.6 volts to 1.8 volts. At 1.8 volts of field telemetry, a positive pulse creates zero change. This demonstrates that no greater field can be achieved. Similarly, at 0.6 volts a negative pulse generates no change. These are the saturation points of the rod. At this point, the Alnico material is fully polarized.

It is easier to de-magnetize the rod than it is to magnetize it. At full saturation (1.8 V) a single negative pulse brings it to almost zero dipole. It then takes at least six further negative pulses to reach negative saturation. This behaviour allows for open loop degaussing where a series of pulses in opposing directions brings the field to zero.

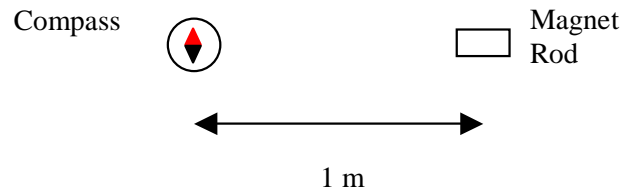


Figure 7: Dipole Measurement Method

Figure 7 shows the very simple apparatus used to measure the dipole moment of the magnet rod. The rod is fully saturated in one direction, and a compass is placed one meter from its center aligned with its long axis. The entire assembly is rotated until the compass needle reads North.

A series of pulses are then sent to the magnet rod to fully saturate it in the opposite direction. Using the LatinSat-B rod, a compass deflection of 21° was obtained. This experiment was conducted at 43.716° N, 79.821° W, 764 feet above sea level, where the horizontal component of the geomagnetic field is 18012 nT (from the online IGRF model⁴).

Making small-angle approximations (reasonable given the general coarseness of the measurement) the magnetic field B due to the rod is:

$$B = 18012 \text{ nT} \cdot \sin\left(\frac{21^\circ}{2}\right)$$

$$B = 3300 \text{ nT}$$

At one meter from the center of the rod, it is assumed that the compass is in the far field. The axial far field for a dipole magnet with strength m is:

$$B = \frac{\mu_0}{4\pi} \cdot \frac{2m}{r^3}$$

Solving for the dipole moment:

$$m = 16.5 \text{ Am}^2$$

This is the greatest dipole that can be created in either direction. For comparison, a magnetic torquer⁵ of equivalent performance has a mass of 430 grams, a length of 33 cm, and a power consumption of 1.11 Watts. The reversible permanent magnet is lighter, shorter and uses far less power, though clearly it has a lower control bandwidth.

Simulations

The attitude dynamics of the LatinSat spacecraft are numerically simulated to obtain an understanding of the expected orbital results. Two scenarios are considered. In one, the reversible permanent magnet maintains a constant dipole. In the other, its polarity is reversed each time the equator is crossed. We model the spacecraft as a rigid body and assume that its rotational dynamics evolve according to Euler's equation:

$$\mathbf{I}\dot{\boldsymbol{\omega}} + \boldsymbol{\omega}^x \mathbf{I}\boldsymbol{\omega} = \mathbf{G} \quad (1)$$

where $\boldsymbol{\omega} = [\omega_1 \ \omega_2 \ \omega_3]^T$ is the absolute angular velocity expressed in a body-fixed frame which is assumed to be a principal-axis frame, \mathbf{I} is the diagonal moment of inertia matrix, and \mathbf{G} is the external torque which is described in more detail below. Given the cubical nature of the satellite, we take the entries in \mathbf{I} to have the identical value of $0.118 \text{ kg} \cdot \text{m}^2$. We have also introduced the notation

$$\boldsymbol{\omega}^x = \begin{bmatrix} 0 & -\omega_3 & \omega_2 \\ \omega_3 & 0 & -\omega_1 \\ -\omega_2 & \omega_1 & 0 \end{bmatrix} \quad (2)$$

In general, we follow the notation of Hughes⁶.

The orientation of the body-fixed frame with respect to the usual geocentric inertial frame is described with the rotation matrix \mathbf{C}_{bi} which can be expressed in terms of the Euler parameters (also known as quaternions) $\boldsymbol{\varepsilon} = [\varepsilon_1 \ \varepsilon_2 \ \varepsilon_3]^T$ and η :

$$\mathbf{C}_{bi} = (\eta^2 - \boldsymbol{\varepsilon}^T \boldsymbol{\varepsilon})\mathbf{1} + 2\boldsymbol{\varepsilon}\boldsymbol{\varepsilon}^T - 2\eta\boldsymbol{\varepsilon}^x \quad (3)$$

The Euler parameters evolve according to the differential equations

$$\begin{aligned} \dot{\boldsymbol{\varepsilon}} &= \frac{1}{2}(\boldsymbol{\varepsilon}^x + \eta \mathbf{1})\boldsymbol{\omega} \\ \dot{\eta} &= -\frac{1}{2}\boldsymbol{\varepsilon}^T \boldsymbol{\omega} \end{aligned} \quad (4)$$

The simulation consists of simultaneously integrating Eqs. (1) and (4) which we perform using a fourth-order Runge-Kutta procedure with a time step of 0.1 seconds.

We also introduce the following notation for principal rotation matrices:

$$\begin{aligned} \mathbf{C}_1(\theta) &= \begin{bmatrix} 1 & 0 & 0 \\ 0 & c_\theta & s_\theta \\ 0 & -s_\theta & c_\theta \end{bmatrix}, \quad \mathbf{C}_2(\theta) = \begin{bmatrix} c_\theta & 0 & -s_\theta \\ 0 & 1 & 0 \\ s_\theta & 0 & c_\theta \end{bmatrix}, \\ \mathbf{C}_3(\theta) &= \begin{bmatrix} c_\theta & s_\theta & 0 \\ -s_\theta & c_\theta & 0 \\ 0 & 0 & 1 \end{bmatrix} \end{aligned} \quad (5)$$

where c and s denote the cosine and sine functions. The spacecraft position components in the geocentric inertial frame, $\mathbf{r} = [r_1 \ r_2 \ r_3]^T$, are given by

$$\mathbf{r} = \mathbf{C}_3^T(\Omega)\mathbf{C}_1^T(i)\mathbf{C}_3^T(\omega) \begin{bmatrix} a \cos \theta \\ a \sin \theta \\ 0 \end{bmatrix} \quad (6)$$

Here, $\Omega = 90$ deg is the longitude of the ascending node, $i = 65$ deg is the inclination, $\omega = 0$ is the argument of perigee, $a = 7028$ km is the orbit radius, and $\theta = nt$ is the true anomaly. The mean motion (angular rate) of the orbit is $n = \sqrt{\mu/a^3}$ where μ is the geocentric gravitational constant. Given the spacecraft position, the components of the Earth's magnetic field may be determined in the inertial frame. Here, we use the magnetic dipole model given by Wertz⁷:

$$\mathbf{B}_i = \begin{bmatrix} (B_r \cos \delta + B_\theta \sin \delta) \cos \alpha - B_\phi \sin \alpha \\ (B_r \cos \delta + B_\theta \sin \delta) \sin \alpha - B_\phi \cos \alpha \\ B_r \sin \delta - B_\theta \cos \delta \end{bmatrix}$$

where α and δ are the spacecraft right ascension and declination, respectively. The geomagnetic field components in spherical coordinates are given by

$$\begin{aligned} B_r &= 2 \left(\frac{a_e}{r} \right)^3 [g_1^0 \cos \theta_m + (g_1^1 \cos \theta_m + h_1^1 \sin \phi_m) \sin \theta_m] \\ B_\theta &= \left(\frac{a_e}{r} \right)^3 [g_1^0 \sin \theta_m - (g_1^1 \cos \theta_m + h_1^1 \sin \phi_m) \cos \theta_m] \\ B_\phi &= \left(\frac{a_e}{r} \right)^3 [g_1^1 \sin \phi_m - h_1^1 \cos \phi_m] \end{aligned}$$

where θ_m and ϕ_m are the co-elevation and east-longitude of the spacecraft, a_e is the radius of the earth, and g_1^0 , g_1^1 , and h_1^1 are geomagnetic field coefficients.

The components of the magnetic field can be expressed in the body-fixed frame according to $\mathbf{B}_b = \mathbf{C}_{bi}\mathbf{B}_i$.

The external torques acting on the spacecraft are assumed to emanate from three sources: the magnetic torque \mathbf{G}_m due to the on-board dipole moment which we denote by $\mathbf{m} = [m_1 \ m_2 \ m_3]^T$, the torque due to the magnetic hysteresis rods \mathbf{G}_h , and the solar pressure torque \mathbf{G}_s . The latter is assumed to accrue from the four pairs of alternating black and silver tape placed along the edges parallel to the Z-axis and visible in Figure 1. Hence, the total torque is given by

$$\mathbf{G} = \mathbf{G}_m + \mathbf{G}_h + \mathbf{G}_s \quad (7)$$

where

$$\begin{aligned} \mathbf{G}_m &= \mathbf{m}^x \mathbf{B}_b \\ \mathbf{G}_h &= k_m \mathbf{B}_b^x \mathbf{B}_b^x \boldsymbol{\omega} \\ \mathbf{G}_s &= \sum_{i=1}^8 \mathbf{G}_{si} \end{aligned} \quad (9)$$

The value of the magnetic hysteresis constant is taken as $k_m = 10^6 \text{ N} \cdot \text{m} \cdot \text{s} / \text{T}^2$. In addition, \mathbf{G}_{si} is the solar pressure torque produced by the i th surface. We have $\mathbf{G}_{si} = \mathbf{r}_i^x \mathbf{F}_{si}$ where \mathbf{r}_i is the centroid of the i th surface (assumed to be the center of pressure) and \mathbf{F}_{si} is the corresponding solar pressure force. It is given by

$$\mathbf{F}_{si} = pA_i(\mathbf{n}_i^T \mathbf{s}_b)[\rho_{ai}\mathbf{s}_b + 2\rho_{si}\mathbf{n}_i], \quad \mathbf{n}_i^T \mathbf{s}_b > 0$$

where p is the solar pressure constant, A_i is the surface area, ρ_{ai} is the fraction of the solar radiation that is absorbed, ρ_{si} is the fraction that is (specularly) reflected, \mathbf{n}_i is a unit vector in the direction of the inward normal to the surface, and \mathbf{s}_b is the direction of the sun's rays expressed in the body-fixed frame. If $\mathbf{n}_i^T \mathbf{s}_b < 0$ then $\mathbf{F}_{si} = \mathbf{0}$ since the surface receives no solar radiation. For the black strips, we take $\rho_{ai} = 0.97$ and $\rho_{si} = 0.03$ and for the silver strips, $\rho_{ai} = 0.08$ and $\rho_{si} = 0.92$.

In order to visualize the attitude motion of the spacecraft, we would like to describe its orientation with respect to the standard roll-pitch-yaw frame. In this frame, the 3-axis points toward the earth, the 1-axis points along the spacecraft orbital velocity vector and the 2-axis points in the opposite direction to the orbit normal. If \mathbf{C}_{bo} denotes the corresponding rotation matrix and \mathbf{C}_{oi} is the rotation matrix relating the orbital frame to the inertial frame, then $\mathbf{C}_{bi} = \mathbf{C}_{bo}\mathbf{C}_{oi}$ where

$$\mathbf{C}_{oi} = \mathbf{C}_o \mathbf{C}_3(\omega + \theta) \mathbf{C}_1(i) \mathbf{C}_3(\Omega),$$

$$\mathbf{C}_o = \begin{bmatrix} 0 & 1 & 0 \\ 0 & 0 & -1 \\ -1 & 0 & 0 \end{bmatrix}$$

If we opt to describe \mathbf{C}_{bo} using the standard yaw-pitch-roll (3-2-1) Euler angle sequence then

$$\mathbf{C}_{bo} = \mathbf{C}_{bi} \mathbf{C}_{oi}^T = \mathbf{C}_1(\theta_1) \mathbf{C}_2(\theta_2) \mathbf{C}_3(\theta_3)$$

from which θ_1 , θ_2 , and θ_3 can be extracted.

For our simulations, we take for initial conditions $\boldsymbol{\epsilon}(0) = \mathbf{0}, \eta(0) = 1, \omega_1(0) = \omega_2(0) = 0$, and $\omega_3(0) = -0.035 \text{ rad/s}$. The latter value matches the flight results for the spin rate obtained from the solar array currents. The results from two simulations will be presented. In the first simulation, the magnetic dipole moment due to the permanent magnet ($5 \text{ A} \cdot \text{m}^2$) and the magnetic actuator is taken to be

$$m_1 = 0, m_2 = 0, m_3 = 18 \text{ A} \cdot \text{m}^2$$

In the second simulation we take

$$m_1 = 0, m_2 = 0, m_3 = \begin{cases} 18 \text{ A} \cdot \text{m}^2, & r_3 \geq 0 \\ -8 \text{ A} \cdot \text{m}^2, & r_3 < 0 \end{cases}$$

This corresponds to toggling the magnetic dipole moment of the magnetic actuator from $+13 \text{ A} \cdot \text{m}^2$ to $-13 \text{ A} \cdot \text{m}^2$ when crossing from the northern hemisphere to the southern hemisphere.

The simulation results for Simulation 1 are given in Figure 8 where we have plotted the Euler angles and spacecraft angular velocities for one orbit. Examination of the roll and pitch angles reveals a roughly earth-pointing situation with the +Z-face facing the earth over the first half of the orbit (northern hemisphere) and the -Z-face facing the earth over the second half of the orbit (southern hemisphere). The roll angle clearly shows the turn made by the spacecraft when crossing (magnetic) hemispheres which is expected. The best pointing is accomplished in the vicinity of the poles.

The results of Simulation 2 are given in Figure 9. In this case, the roll and pitch angles indicate that the same face of the spacecraft, namely the +Z-face, remains roughly earth-pointing. Although the reversal of the magnetic dipole moment creates a transient disturbance when the equator is crossed, the roll reversal shown in Simulation 1 does not occur. An interesting prediction of the simulation is the reversal of the sign of the spin rate about the Z-axis.

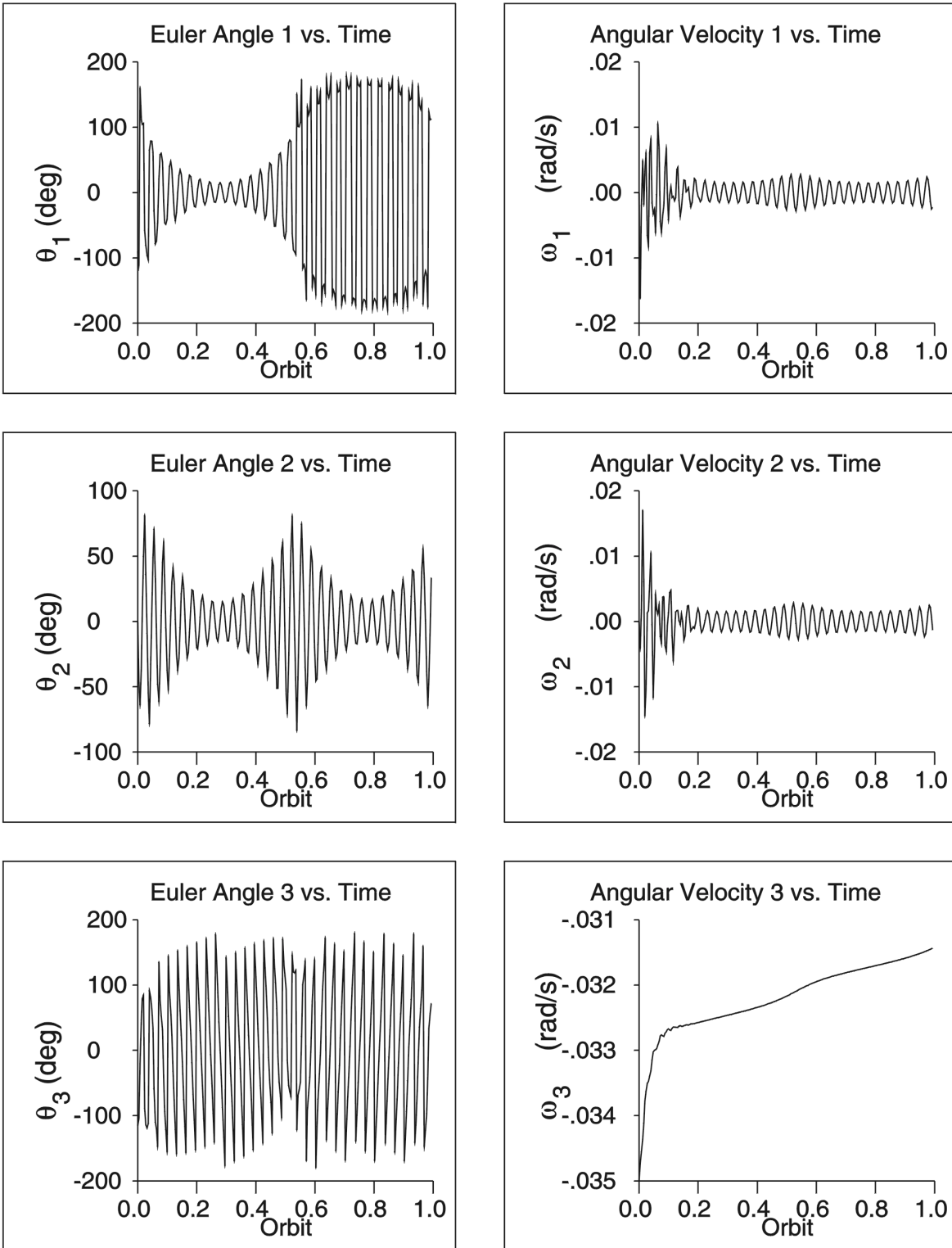


Figure 8: Simulation Results 1 (Constant Dipole)

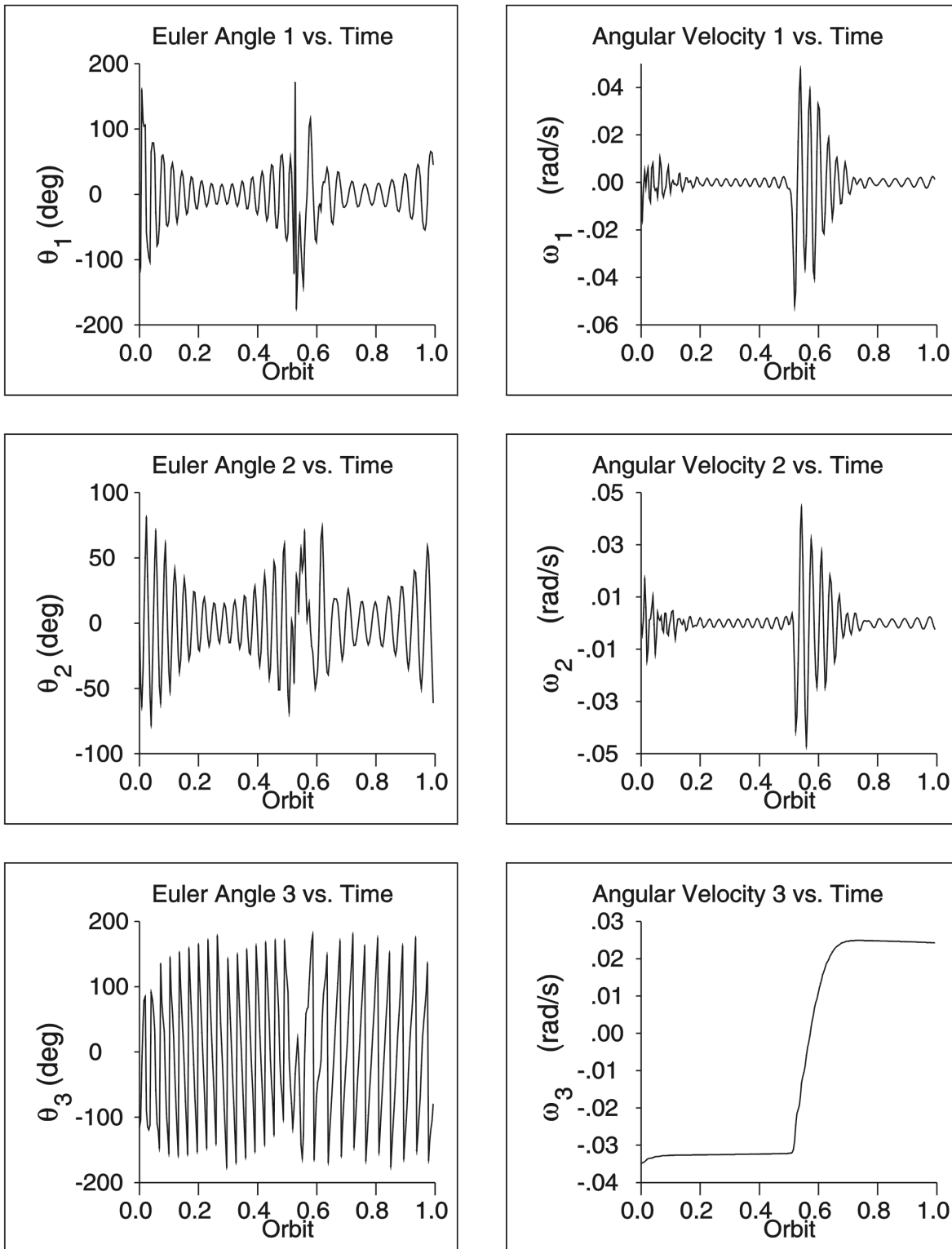


Figure 9: Simulation Results 2 (Toggled Dipole)

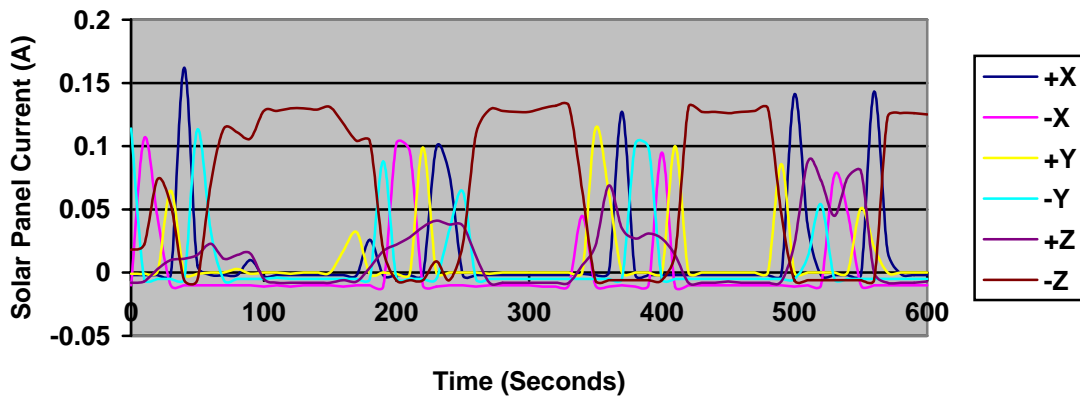


Figure 10: Orbital Data from January 16, 2003

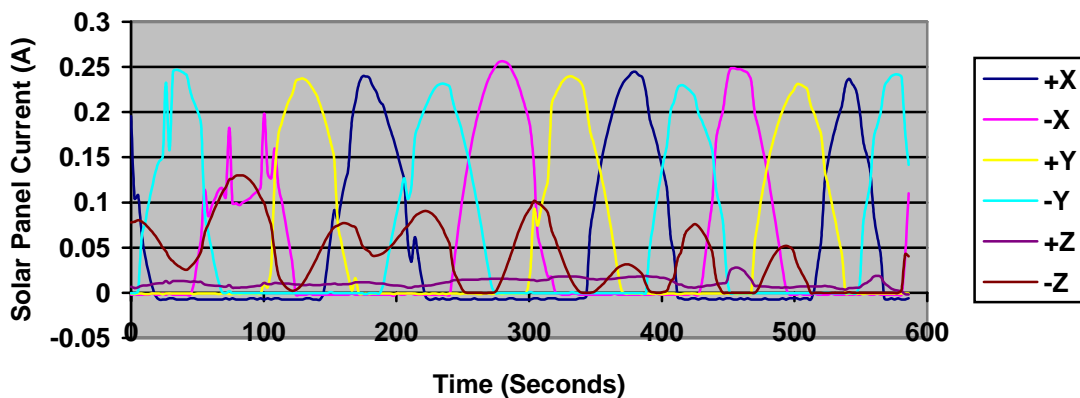


Figure 11: Orbital Data from April 4, 2003

Orbital Results

The two figures above show solar array current telemetry for LatinSat-B. This can be used as a simple sun-sensor, to determine the attitude motion of the spacecraft.

The Figure 10 data was collected 29 days after launch. From the X and Y solar arrays, it can be seen that the satellite is spinning with a period of approximately one minute. There is also a large precession motion, as evidenced by the currents seen on the Z solar panels. Sometimes the $-Z$ array is fully illuminated, while at other times the $+Z$ array sees some sunlight. This suggests a nutation angle of greater than 45° . The precession period is approximately 160 seconds.

The Figure 11 data shows the satellite's motion more than three months after launch. The spin rate, while in the same direction, has slowed to one rotation every three minutes. The nutation angle is very significantly reduced. At this point the satellite has settled down into its steady state.

Commissioning of the LatinSat-B magnetometer and inertial sensors is ongoing. These sensors will be used to observe the satellite motion in detail so that the precise kinematics of the flip may be investigated. The reversible permanent magnet actuator has not yet been used to flip either of the LatinSats. However, the high-voltage supply has been turned on, and the results are consistent with pre-launch testing. There is every expectation that by the time this paper is published, the actuator will have been used to reverse the orientation of LatinSat-B and the kinematics results observed.

Ongoing Developments

Sinclair Interplanetary continues to develop the reversible permanent magnet technology, and is proceeding along a number of promising paths. These are: pulse duration control, multi-axis packaging, and composite soft/hard-iron cores.

Drive electronics with pulse duration control are presently at the qualification model stage and await a suitable launch opportunity. The thyristor switches of the previous generation are replaced by Insulated-Gate Bipolar Transistors (IGBTs). These parts add the capability to end a discharge before the capacitor is empty. Indeed, the bridge is configured so that the remaining inductive energy in the rod is returned to the capacitor for use in the next pulse. Average power consumption is reduced, and the maximum pulse rate is increased enabling higher bandwidth control.

Multi-axis packaging allows an arbitrary dipole vector to be produced in three dimensions. The magnet rods can be much shorter than comparable magnetic torquers, so less space is wasted putting three orthogonal rods in a common box. A number of rods could share a single high voltage supply and capacitor.

Finally, magnet cores made from a combination of hard and soft iron are of some interest. The hard iron alloy (Alnico) can be permanently magnetized, but saturates at approximately 1 tesla. Soft iron alloys saturate at roughly twice the field. It should be possible to fit soft iron pole-pieces to the Alnico to increase the dipole-to-mass ratio of the system.

There may be other uses for this technology besides flipping magnetically stabilized satellites. A magnet rod might be used as a safe-hold actuator. In normal operations, the rod would have no dipole and the spacecraft would be 3-axis controlled by reaction wheels. In the event of an anomaly, a dipole could be generated to magnetically stabilize the satellite until the regular ACS is restored.

A reversible permanent magnet might also be useful as a trim magnet on a 3-axis controlled satellite. In low Earth orbit, the primary attitude disturbance torque tends to be magnetic. If the satellite's dipole could be nulled dynamically on-orbit the rest of the ACS could be made smaller and simpler.

Conclusion

Preliminary on-orbit results show that the LatinSat spacecraft have successfully aligned themselves with the geomagnetic field. Their motion is similar to that of the many magnetically stabilized satellites that have gone before them. One set of antennas can be used over the Northern Hemisphere, and the other over the Southern Hemisphere.

The unique magnetic actuator will allow the satellites to be inverted. When fired at each equator crossing, it has the potential to keep one face continually towards the Earth. Numerical simulations also show an unexpected behaviour. As the satellite actuates the magnet, its spin direction will reverse. This hypothesis will be tested immediately after the first magnet firing.

A third reversible permanent magnet from the LatinSat build lot has been integrated with AMSAT-OSCAR-E. This satellite uses a SpaceQuest microsat bus, and should behave in a similar manner to the LatinSats. Its launch is expected in May of 2004.

The next generation of reversible permanent magnets is presently undergoing qualification testing. The interface is compatible with previous models, but this version offers lower power consumption and greater control bandwidth. Several flight opportunities are being pursued, but it has not yet been manifested. Looking further ahead, Sinclair Interplanetary intends to continue to advance this technology, providing a new ACS option to the microsatellite community.

Acknowledgments

The authors would like to thank Dino Lorenzini, Mark Kanawati, Glenn Richardson, and the rest of the SpaceQuest team for providing this flight opportunity. Thanks also to Jan King, project manager for Australis-OSCAR-5, for his insights into the history of spacecraft magnetic control.

References

- ¹ CRC Handbook of Chemistry and Physics, 49th edition, The Chemical Rubber Company, Cleveland, 1968.
- ² King, J. A., e-mail communication.
- ³ White, J., "Microsat Motion, Stabilization, and Telemetry (and why we care about it)." Proceedings of the AMSAT-NA International Space Symposium, November 1990.
- ⁴ <http://www.ngdc.noaa.gov/cgi-bin/seg/gmag/fldsnt1.pl>
- ⁵ Microcosm Space Mission Engineering, part number MT-15-1 technical information.
- ⁶ Hughes, P. C., Spacecraft Attitude Dynamics, John Wiley, Toronto, 1986.
- ⁷ Wertz, J. R., Spacecraft Attitude Determination and Control, Kluwer, Dordrecht, 1978.